applied optics

Design of superachromatic quarter-wave retarders in a broad spectral range

Jose Maria Herrera-Fernandez,[1,*] Jose Luis Vilas,[2] Luis Miguel Sanchez-Brea,[1] and Eusebio Bernabeu[1]

[1]Optics Department, Applied Optics Complutense Group, Universidad Complutense de Madrid (UCM), Facultad de Ciencias Fisicas, Plaza de las Ciencias 1, 28040, Madrid, Spain
[2]Biocomputing Unit, Centro Nacional de Biotecnologia-CSIC, Darwin, 3, 28049, Cantoblanco, Madrid, Spain
*Corresponding author: josemariahf@fis.ucm.es

Received 25 August 2015; revised 20 October 2015; accepted 20 October 2015; posted 21 October 2015 (Doc. ID 248353); published 00 MONTH 0000

A superachromatic quarter-wave retarder using an arbitrary number of waveplates in a broadband spectral range has been proposed. Their design is based on the optimization of a merit function, the achromatism degree (*AcD*), which represents a global behavior metric for the retardation. By means of this technique, the thickness and azimuth of each waveplate is determined. The achromatism degree is a measure of the distance between the overall retardation and a target retardation weighted by the spectrum of the incident light. We report on a particular case where all waveplates are made of quartz. As application examples, the design of a quarter-wave retarder using two, three, and four waveplates in the spectral ranges of 500–700 nm and 400–1000 nm was studied. The numerical results show that for these ranges, the best designs obtained present a maximum difference of 0.013° and 0.010° with respect to the target retardation, respectively. In addition, an analysis of their achromatic stability is presented. These results can be applied in the aerospace industry, spectroscopic ellipsometry, and spectrogoniometry, among others. © 2016 Optical Society of America

OCIS codes: (220.4830) Systems design; (260.5430) Polarization; (260.1440) Birefringence; (160.1190) Anisotropic optical materials.

http://dx.doi.org/10.1364/AO.99.099999

1. INTRODUCTION

High-purity polarized light is essential in numerous experiments and applications [1,2]. To obtain polarized light, linear polarizers [3], birefringence waveplates [4], and Fresnel rhombs [5], among others, can be used. Since the beginning of linear mathematical representations of optical systems carried out by Jones and Mueller [6,7], the design of achromatic configurations, that is, the capability of working properly inside a broad spectral range, has been deeply analyzed. Pancharatnam showed the possibility of obtaining an achromatic system using three birefringent plates of the same material placed in a cascade, and by establishing conditions in the retardation and the orientation of waveplates (Pancharatnam's type). Therefore, the system behaves as an equivalent retarder element in a wide spectral range [4]. Using this idea, several works have been proposed where the achromatic system is formed with only a couple of waveplates [8,9,10]. Afterward, Hariharan pointed out how achromatic configurations can be achieved by imposing contour conditions with two waveplates of different materials and specific thicknesses [11], and how to choose the materials of the waveplates [12]. Recently, some techniques have been suggested in order to improve the achromatism. For instance, one work combined two twisted nematic liquid-crystal cells where the material dispersion is considered [13], while another used stacks of thin films, which also allows the design of a uniform phase delay in both the passband and stopband [14] through the imitation of biological structures as the eyes of stomatopod crustaceans, which inspired the creation of periodically multilayered structures comprising two different types of arrays of nanorods [15], etc. However, these methods are generally expensive and difficult to carry out.

Another possibility to design achromatic systems is the use of subwavelength gratings. When the period of a diffraction grating is smaller than the wavelengths of the incident light, the grating can be considered an optically anisotropic medium [16,17]. An alternative way is to provide more degrees of freedom to the achromatic system by increasing the number of waveplates. Masson proposed an achromatic system with six waveplates, where the thickness and the angle of each quartz plane is optimized [18]. Ma applied a simulated annealing algorithm for designing a multilayer achromatic system with three, six, and ten layers [19]. With the same algorithm, Chen optimizes a nine-piece system through a merit function that incorporates the optical axis and output linearity [20]. Nevertheless, these studies were carried out in the range of terahertz. When studies are focused on the visible range, commercial waveplates (quarter- and half-waveplates) are normally used, and their optimization is limited [21–23].

The aim of this work is to present a simple and accurate technique for the design of superachromatic quarter-wave retarders based on the Jones equivalence theorem, where the equivalent retardation is obtained by using a cascade of waveplates. The superachromatism is achieved by the optimization of the thickness and the angle of the waveplates with respect to the reference axis. The work is divided into several parts. In Section 2, the overall retardation of a system with N waveplates is given through the optimization of the thicknesses and the azimuths when the material is fixed. In Section 3, the numerical results when the chosen material is quartz are evaluated for two wide spectral ranges, including the visible and infrared spectra. Finally, the achromatic stability of the obtained configuration in higher spectral ranges is analyzed in Section 4. The main results are summarized in Section 5.

2. THEORETICAL ANALYSIS

Let us consider the scheme shown in Fig. 1. An optical system M is formed by N waveplates, which are placed in a cascade.

In mathematical terms, M is obtained as the product of N waveplates matrices, $\mathbf{C}_j(\phi_j, \delta_j)$, $j = 1, \ldots, N$, which are characterized by their retardations δ_j and the azimuths of their fast axis ϕ_j with respect to the reference axis. Without loss of generality, the fast axis of the first plate will be defined as reference axis $\phi_1 = 0$; therefore, the angles ϕ_j represent the angle between the fast axis of the first waveplate and the fast axis of the waveplate in position j. Moreover, the system is immersed in air, illuminated with a spectrum $g(\lambda)$, and the incidence angle is normal to each waveplate. Thus,

$$M = \mathbf{C}_N(\phi_N, \delta_N) \cdots \mathbf{C}_1(\phi_1, \delta_1) = \prod_j \mathbf{C}_j(\phi_j, \delta_j). \tag{1}$$

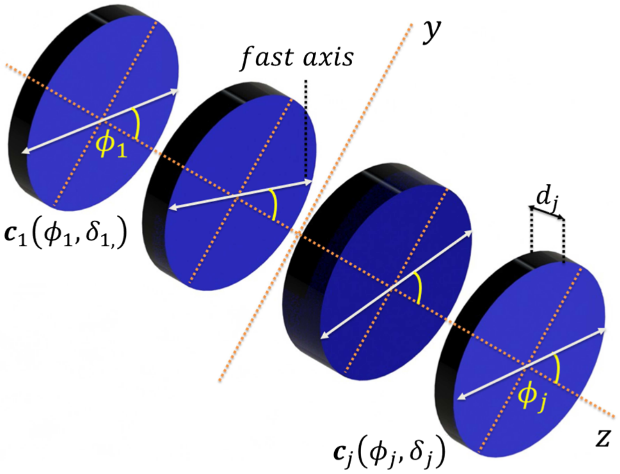

Fig. 1. Scheme of system M under studio. A set of N waveplates of the same material is placed in a cascade configuration. $\mathbf{C}_j(\phi_j, \delta_j)$ is the matrix of the j-th waveplate, where ϕ_j is the azimuth, δ_j is the retardation, and d_j is the thickness.

The retardation of each waveplate is defined by

$$\delta_j = \frac{2\pi \Delta n}{\lambda} d_j, \tag{2}$$

where λ represents the incident wavelength, d_j represents the thickness of the each waveplate, and the difference $\Delta n = n_e - n_o$ is the birefringence of the material, n_e and n_o being the extraordinary and ordinary refractive indexes of the material, respectively. Thus, the matrix of each waveplate is given by

$$C(\phi_j, \delta_j) = \begin{pmatrix} \cos\frac{\delta_j}{2} + i \sin\frac{\delta_j}{2} \cos 2\phi_j & i \sin\frac{\delta_j}{2} \sin 2\phi_j \\ i \sin\frac{\delta_j}{2} \sin 2\phi_j & \cos\frac{\delta_j}{2} - i \sin\frac{\delta_j}{2} \cos 2\phi_j \end{pmatrix}, \tag{3}$$

where i is the imaginary unit. Since matrices $\mathbf{C}(\phi_j, \delta_j)$ are unitary, the product matrix is unitary and defined by

$$M = \begin{pmatrix} A & B \\ -B^* & A^* \end{pmatrix}, \tag{4}$$

where the symbol X^* denotes the complex conjugate of X, and $A = A(\phi_j, \delta_j)$ and $B = B(\phi_j, \delta_j)$ are complex expressions. Therefore, according to the equivalence theorem [24], every unitary matrix can be decomposed by the product of a rotator and a retarder, that is, $M = R(\Psi)C(\theta, \Delta)$. Thus, the overall retardation of the system, Δ, can be obtained as follows [18,25]:

$$\tan^2 \frac{\Delta}{2} = \frac{\mathrm{Im}(A)^2 + \mathrm{Im}(B)^2}{\mathrm{Re}(A)^2 + \mathrm{Re}(B)^2}. \tag{5}$$

The expressions for the equivalent azimuth, Ψ, and the rotation angle, θ, will not be used in the optimization. In order to obtain an achromatic retarder in a certain spectral range, the overall retardation, Δ, should be constant and independent of the wavelength. However, that is an unrealistic situation. Thus, the goal of the designing of an achromatic retarder is to achieve a very flat retardation curve that can be approximated by a constant line. The achromatic performance of an optical system in a spectral interval can be measured using the *achromatism degree* (AcD) [26]. However, in our work, a redefinition of the AcD is presented due to simplicity; thus, with the redefinition, the unit of AcD is given simply in degrees. This merit function is defined as the difference between the overall retardation of the system, Δ, and a target retardation, Δ_0, weighed by the spectrum $g(\lambda)$ as follows:

$$AcD = \frac{\sqrt{\int_\Omega |\Delta - \Delta_0|^2 g(\lambda) \mathrm{d}\lambda}}{\sqrt{\int_\Omega g(\lambda) \mathrm{d}\lambda}}, \tag{6}$$

where Ω represents an interval of wavelengths, i.e., the spectral range. As a consequence, $AcD \geq 0$ is equally null when the system is absolutely achromatic, and $\Delta = \Delta_0 = cte$. Therefore, the maximum achromatism is achieved when the value of AcD is at its minimum. For a system composed by a set of N waveplates, AcD will depend on the thicknesses $\vec{d} = (d_1, d_2, \ldots, d_N)$, the materials $\overrightarrow{\Delta n} = (\Delta n_1, \Delta n_2, \ldots, \Delta n_N)$, and the azimuths $\vec{\phi} = (0, \phi_2, \phi_3, \ldots, \phi_N)$ of the waveplates, that is, $AcD = AcD(\vec{d}, \vec{\phi}, \overrightarrow{\Delta n})$. Note that $\phi_1 = 0$ is the reference axis. Therefore, an optimization of the AcD through the azimuth, thickness, or material of the waveplates can be used to obtain an achromatic configuration. Since the birefringence of the materials presents a complex dependence with the wavelength given, for example, by the Sellmeier relation, the optimization of the material increases the complexity of numerical analysis [27]. For this reason, an optimization using only azimuths and thicknesses will be carried out.

3. NUMERICAL RESULTS AND DISCUSSION

In this section, the interesting case where all waveplates are made of quartz is studied. The use of this material, which is widely used in many industries, such as the aerospace industry, is due to its excellent optical properties [27,28] and low cost. Note that although in this analysis, a plane spectrum has been used as the incident light, $g(\lambda) = \text{constant} = 1$, more complex spectra can be considered without loss of validity in the results presented. Under this hypothesis, Eq. (6) can be minimized using the thicknesses $\vec{d}$ and the azimuths $\vec{\phi}$. The value of the employed birefringence for the quartz has been taken from Ghosh [27]:

$$n_o^2 - 1 = \frac{0.663044)\lambda^2}{\lambda^2 - (0.0600)^2} + \frac{0.517852\lambda^2}{\lambda^2 - 0.1060^2} + \frac{0.175912\lambda^2}{\lambda^2 - 0.1190^2} + \frac{0.565380\lambda^2}{\lambda^2 - 8.844^2} + \frac{1.675299\lambda^2}{\lambda^2 - 20.742^2}, \tag{7}$$

$$n_e^2 - 1 = \frac{0.665721\lambda^2}{\lambda^2 - 0.0600^2} + \frac{0.503511\lambda^2}{\lambda^2 - 0.1060^2} + \frac{0.214792\lambda^2}{\lambda^2 - 0.1190^2} + \frac{0.539173\lambda^2}{\lambda^2 - 8.792^2} + \frac{1.8076613\lambda^2}{\lambda^2 - 19.70^2}. \tag{8}$$

Also, we have assumed that the medium wherein the system is immersed is air. The transmittance of surfaces should also be considered using Fresnel coefficients in order to determine the energy losses. Nevertheless, in normal incidence, the transmission at the surface does not change the state of polarization, and is not relevant for our analysis. To improve energy losses, an anti-reflection coating on the surface can be used.

Several minimization processes of AcD for the configurations composed by two, three, and four waveplates in the spectral ranges of 500–700 nm and 400–1000 nm have been performed. We have chosen these ranges due to their particular use in the field of optics. However, the use of other spectral ranges is possible. The aim was to achieve a quarter-wave super-achromatic retarder illuminated with a flat spectrum, therefore, $\Delta_0 = \pi/2$. Other achromatic wave retarders λ/N can be obtained by changing the target retardation. As an optimization tool, the simplex search method of Lagarias *et al.* has been used [29]. This method is implemented in MATLAB software with the fminsearch algorithm, which finds the minimum of the unconstrained multivariable function using the derivative-free method [30]. In order to find the best possible parameters, each simulation of the achromatic system has been repeated with different random seeds at least 1000 times. In Table 1, the optimal thicknesses and azimuths of the waveplates obtained for each achromatic configuration are shown. In particular, for the spectral range 400–1000 nm, the best result, $AcD = 0.038°$, is achieved for the system with four waveplates, and $d_1 = 30.7$ µm, $d_2 = 92.1$ µm, $d_3 = 30.7$ µm, $d_4 = 46.0$ µm,

Table 1. Optimized parameters for the achromatic systems with $N = 2, 3$, and 4 waveplates and two different wavelength range[a]

N	400–1000 nm	500–700 nm
2	$d_1 = 15.7$ µm	$d_1 = 31.0$ µm
	$d_2 = 31.2$ µm	$d_2 = 16.0$ µm
	$\phi_2 = 54.1°$	$\phi_2 = 59.1°$
	$AcD = 3.67°$	$AcD = 0.20°$
	$f_2^{400\text{–}1000} = 19.74°$	$f_2^{500\text{–}700} = 1.07°$
3	$d_1 = 15.4$ µm	$d_1 = 63.8$ µm
	$d_2 = 61.8$ µm	$d_2 = 95.7$ µm
	$d_3 = 30.9$ µm	$d_3 = 15.9$ µm
	$\phi_2 = 69.6°$	$\phi_2 = 86.0°$
	$\phi_3 = 2.5°$	$\phi_3 = 34.5°$
	$AcD = 0.28°$	$AcD = 0.0018°$
	$f_3^{400\text{–}1000} = 2.08°$	$f_3^{500\text{–}700} = 0.013°$
4	$d_1 = 30.7$ µm	$d_1 = 275.3$ µm
	$d_2 = 92.1$ µm	$d_2 = 212.3$ µm
	$d_3 = 30.7$ µm	$d_3 = 94.4$ µm
	$d_4 = 46.0$ µm	$d_4 = 15.7$ µm
	$\phi_2 = 109.4°$	$\boldsymbol{\phi_2 = 90.0°}$
	$\phi_3 = 35.3°$	$\phi_3 = 86.0°$
	$\phi_4 = 87.7°$	$\phi_4 = 34.5°$
	$AcD = 0.030°$	$AcD = 0.0015°$
	$f_4^{400\text{–}1000} = 0.22°$	$f_4^{500\text{–}700} = 0.0096°$

[a] d_j and ϕ_j are the thickness and the azimuth of the j waveplate, AcD is the achromatism degree of the optimized configuration and f_N^{Ω} is the maximum fluctuation of the overall retardation Δ. $\phi_1 = 0°$ is the reference axis and the order of the wave plates of the system is given by the matrix product, Eq. (1).

$\phi_2 = 109.4°$, $\phi_3 = 35.3°$, and $\phi_4 = 87.7°$, while for the configurations of the three and two waveplates are $AcD = 0.28°$ and $AcD = 3.67°$, respectively. Note that the order of the wave plates of the system is given by the matrix product, Eq. (1). Therefore, the achromatic system with four waveplates improves one and two orders of magnitude over the configurations of three and two waveplates in this spectral range, respectively. The overall retardation versus wavelength for $N = 4$ and $N = 3$ waveplates with the optimized parameters of Table 1 is shown in Fig. 2(a). In order to determine the maximum fluctuation of the retardation, we have used the parameter f_N^{Ω}, which is defined as

$$f_N^{\Omega} = \max_{\Omega}(\Delta) - \min_{\Omega}(\Delta), \tag{9}$$

where Ω is the evaluated spectral range, N is the number of waveplates of the system M, and max and min are the global maximum and the global minimum of the overall retardation Δ in Ω. When $N = 3$, Δ fluctuates between a maximum value of 91.28° and a minimum value of 89.20°, that is, $f_3^{400\text{–}1000} = 2.08°$. When $N = 4$, the fluctuation is between 90.08° and 89.86°, so $f_4^{400\text{–}1000} = 0.22°$. When the spectral range is limited to 500–700 nm, the method is able to decrease the value of AcD by two and three orders of magnitude, achieving an achromatism degree of 0.0018° and 0.0015° for the configurations with $N = 3$ and $N = 4$ waveplates, respectively. In this case, there are no large differences between the configurations of $N = 3$ and $N = 4$; the overall variations are $f_3^{500\text{–}700} = 0.013°$ and $f_4^{500\text{–}700} = 0.0096°$, respectively [Fig. 2(b)]. Therefore, the choice of one combination or another depends

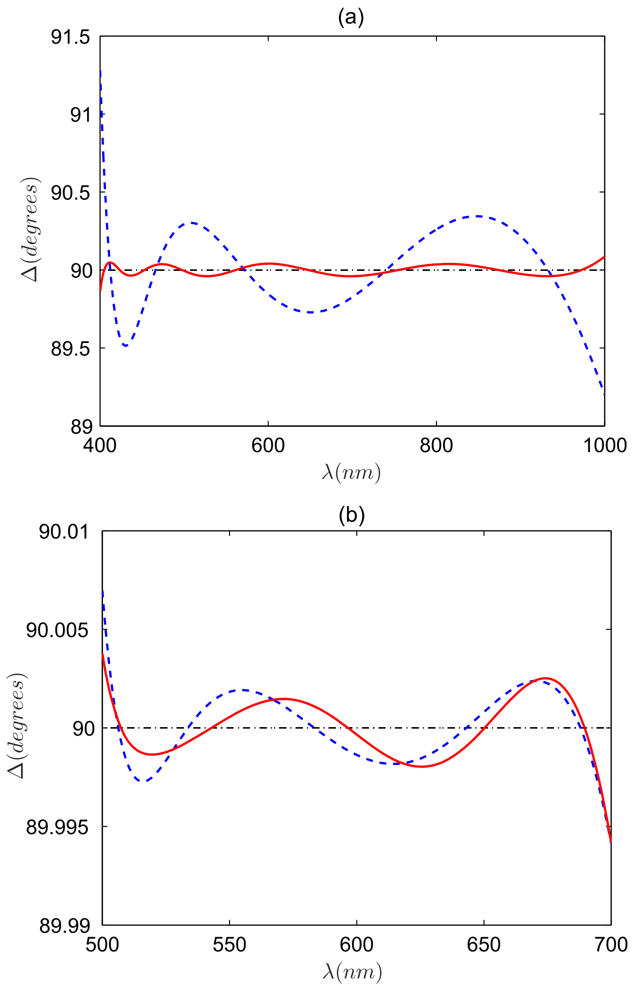

Fig. 2. Overall retardation Δ versus wavelength λ with the configurations of the $N = 3$ (dashed line) and $N = 4$ (solid line) waveplates and the optimization parameters shown in Table 1 for (a) a spectral range of 400–1000 nm and (b) a spectral range of 500–700 nm.

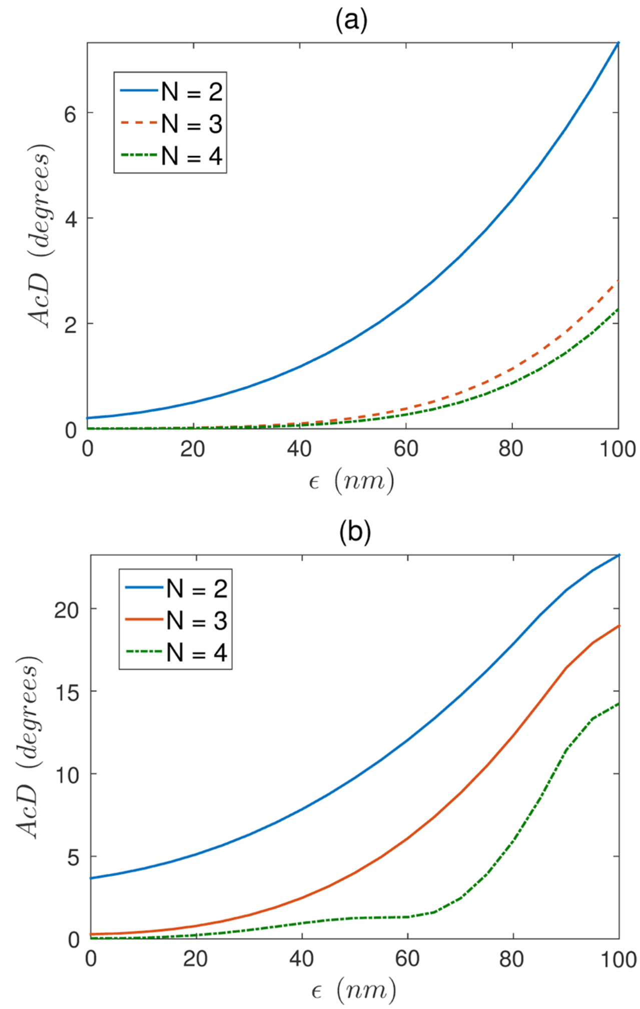

Fig. 3. Stability of AcD for the optimized configuration in both spectral ranges (a) 500–700 nm, and (b) 400–1000 nm, with the configurations of $N = 2$ (line with small dashes), $N = 3$ (line with longer dashes) and $N = 4$ (dashed–dotted line). The waveplates use the optimal parameters shown in Table 1.

on the space requirements of the system. These results represent an improvement of two orders of magnitude over previous works [21–23].

4. STABILITY OF *ACD*

Another important aspect to consider is the tolerances of the achromatic systems obtained in the previous section when the wavelength range is different from the spectral range of the design. Therefore, in this section, the stability of the AcD using the optimal parameters is discussed for higher intervals of wavelengths. Since $|\Delta - \Delta_0|^2 g(\lambda) \geq 0$, then $AcD \geq 0$ for all λ, and as a consequence, when Ω_1 and Ω_2 are two spectral intervals such as $\Omega_1 \subset \Omega_2$, then $AcD(\vec{d}, \vec{\phi})_{\Omega_1} \leq AcD(\vec{d}, \vec{\phi})_{\Omega_2}$. If c_1 is the center of the interval Ω_1 and r_1 its radio, i.e., $\Omega_1 = [c_1 - r_1, c_1 + r_1]$, then the stability of AcD can be analyzed by taking higher intervals, $[c_1 - r_1 - \epsilon, c_1 + r_1 + \epsilon]$, and plotting the AcD in terms of ϵ, ϵ being the extra radio of the higher intervals. This property has been verified in both spectral ranges. In the first one, $\Omega_1 = [500, 700]$ since $\Omega_2 = [300, 900]$, and in the second one, $\Omega_1' = [400, 1000]$ and $\Omega_2' = [300, 1100]$; also, $\epsilon = 200$ nm and $\epsilon = 100$ nm, respectively. In Fig. 3, the stabilities for both cases are shown. When the spectral range is $\Omega_1 = [500, 700]$, the stability of the systems with $N = 3$ (dashed red line) and $N = 4$ (dashed green line) are quite similar. In fact, for $\epsilon \leq 20$ nm, both stabilities are equal, whereas for $\epsilon > 20$ nm, the stability for $N = 4$ is the highest. It is the maximum difference between the global maximum of both functions, 0.54°. Unlike the previous range, when the spectral range is $\Omega_1' = [400, 1000]$, the configuration with $N = 4$ is always the most stable: it is $AcD < 1.6°$ for $\epsilon < 10$ nm.

5. CONCLUSIONS

In this work, superachromatic quarter-wave retarders in a broad spectral range have been designed by means of an arbitrary number of quartz waveplates. The thicknesses and azimuths of the waveplates are obtained by optimizing the achromatism degree, AcD. As an example, this optimization has been carried out for a set of waveplates made of quartz in two spectral ranges, 400–1000 nm and 500–700 nm, for a plane spectrum. The best simulated achromatic configurations are obtained when the system consists of four waveplates in both spectral ranges, with a maximum fluctuation of the overall retardation Δ in the aforementioned spectral ranges of $f_4^{400-1000} = 0.22°$ and $f_4^{500-700} = 0.0096°$, respectively. These values represent remarkable results in superachromatic configurations inside those spectral ranges. In addition, the stability of the achromatic behavior of the configuration has been analyzed for higher intervals of wavelengths in both spectral ranges. The stability grows when the number of waveplates is increased. In particular, the configurations with $N = 4$ waveplates represent a remarkable result in both achromatic retardation and stability.

Funding. Dirección General de Universidades e Investigación, Comunidad de Madrid (Spain) (SEGVAUTOTRIES CM S2013/MIT-2713); Ministerio de Economía y Competitividad (MINECO) (DPI2011-27851).

Acknowledgment. The authors thank Maite Irigoyen for her encouragement and many useful comments during the preparation of this work.

REFERENCES

1. D. H. Goldstein, *Polarized light* (CRC Press, 2010).
2. D. Clarke and J. F. Grainger, *Polarized Light and Optical Measurement: International Series of Monographs in Natural Philosophy* (Elsevier, 2013), vol. **35**.
3. D. S. Kliger and J. W. Lewis, *Polarized light in optics and spectroscopy* (Elsevier, 2012).
4. S. Pancharatnam, "Achromatic combinations of birefringent plates," in Proc. Indian Acad. Sci. A **41**, 137–144 (1955).
5. R. King, "Quarter-wave retardation systems based on the fresnel rhomb principle," J. Sci. Instrum. **43**, 617–622 (1966).
6. R. C. Jones, "A new calculus for the treatment of optical systems," J. Opt. Soc. Am. **31**, 488–493 (1941).
7. S. N. Savenkov, "Jones and mueller matrices: structure, symmetry relations and information content," in *Light Scattering Reviews 4* (Springer, 2009), pp. 71–119.
8. P. Violino, "Polariseur circulaire reglable sur une large domaine de longueurs d onde," Revue Optique **44**, 109–114 (1965).
9. D. Clarke, "Achromatic halfwave plates and linear poliarization rotators," J. Mod. Opt. **14**, 343–350 (1967).
10. P. Hariharan and D. Malacara, "A simple achromatic half-wave retarder," J. Mod. Opt. **41**, 15–18 (1994).
11. P. Hariharan, "Achromatic retarders using quartz and mica," Meas. Sci. Technol. **6**, 1078–1079 (1995).
12. P. Hariharan, "Broad-band apochromatic retarders: choice of materials," Opt. Laser Technol. **34**, 509–511 (2002).
13. S. Shen, J. She, and T. Tao, "Optimal design of achromatic true zero-order waveplates using twisted nematic liquid crystal," J. Opt. Soc. Am. A **22**, 961–965 (2005).
14. Y.-J. Jen, M.-J. Lin, S.-K. Yu, and C.-C. Chen, "Extended broadband achromatic reflective-type waveplate," Opt. Lett. **37**, 4296–4298 (2012).
15. Y.-J. Jen, A. Lakhtakia, C.-W. Yu, C.-F. Lin, M.-J. Lin, S.-H. Wang, and J.-R. Lai, "Biologically inspired achromatic waveplates for visible light," Nat. Commun. **2**, 363 (2011).
16. H. Kikuta, Y. Ohira, and K. Iwata, "Achromatic quarter-wave plates using the dispersion of form birefringence," Appl. Opt. **36**, 1566–1572 (1997).
17. D.-E. Yi, Y.-B. Yan, H.-T. Liu, and G.-F. Jin, et al., "Broadband achromatic phase retarder by subwavelength grating," Opt. Commun. **227**, 49–55 (2003).
18. J.-B. Masson and G. Gallot, "Terahertz achromatic quarter-wave plate," Opt. Lett. **31**, 265–267 (2006).
19. J. Ma, J.-S. Wang, C. Denker, and H.-M. Wang, "Optical design of multilayer achromatic waveplate by simulated annealing algorithm," Chin. J. Astron. Astrophys. **8**, 349–361 (2008).
20. Z. Chen, Y. Gong, H. Dong, T. Notake, and H. Minamide, "Terahertz achromatic quarter wave plate: design, fabrication, and characterization," Opt. Commun. **311**, 1–5 (2013).
21. P. Hariharan and P. Ciddor, "Broad-band superachromatic retarders and circular polarizers for the uv, visible and near infrared," J. Mod. Opt. **51**, 2315–2322 (2004).
22. M. Emam-Ismail, "Retardation calculation for achromatic and apochromatic quarter and half wave plates of gypsum based birefringent crystal," Opt. Commun. **283**, 4536–4540 (2010).
23. A. Saha, K. Bhattacharya, and A. K. Chakraborty, "Achromatic quarter-wave plate using crystalline quartz," Appl. Opt. **51**, 1976–1980 (2012).
24. H. Hurwitz, Jr. and R. C. Jones, "A new calculus for the treatment of optical systems," J. Opt. Soc. Am. **31**, 493–495 (1941).
25. J. L. Vilas, E. Bernabeu, L. M. Sanchez-Brea, and R. Espinosa-Luna, "Circularly polarized light with high degree of circularity and low azimuthal error sensitivity," Appl. Opt. **53**, 3393–3398 (2014).
26. J. L. Vilas, L. M. Sanchez-Brea, and E. Bernabeu, "Optimal achromatic wave retarders using two birefringent wave plates," Appl. Opt. **52**, 1892–1896 (2013).
27. G. Ghosh, "Dispersion-equation coefficients for the refractive index and birefringence of calcite and quartz crystals," Opt. Commun. **163**, 95–102 (1999).
28. M. Bass, C. DeCusatis, J. Enoch, V. Lakshminarayanan, G. Li, C. MacDonald, V. Mahajan, and E. Van Stryland, *Handbook of optics*, Optical properties of materials Nonlinear Optics, Quantum Optics (Optical Society of America, 2009), vol. **4**.
29. J. C. Lagarias, J. A. Reeds, M. H. Wright, and P. E. Wright, "Convergence properties of the nelder-mead simplex method in low dimensions," SIAM J. Optim. **9**, 112–147 (1998).
30. MATLABv2014b, "fminsearch," http://es.mathworks.com/help/matlab/ref/fminsearch.html.

Queries

1. AU: Please translate all national center and university names into English.

2. AU: Please check this edit and confirm that it is correct.

3. AU: Please confirm that this edit is correct.

4. AU: The title of this table has been done incorrectly. Please provide a proper title (in headline-style caps) and put the explanation of the symbols as a caption.

5. The funding information for this article has been generated using the information you provided to OSA at the time of article submission. Please check it carefully. If any information needs to be corrected or added, please provide the full name of the funding organization/institution as provided in the FundRef Registry (http://www.crossref.org/fundref/fundref_registry.html).

6. AU: Please provide all author names in place of "et al" for Ref. [17].

7. AU: Please check and confirm that edit made in Ref. [28] is appropriate.